Glycoconjugate Journal 22, 21–26, 2005

Expression of complex-type N-glycans in developmental periods of zebrafish embryo

Tatsuya Takemoto,[1] Shunji Natsuka,[1] Shin-ichi Nakakita[2] and Sumihiro Hase[1]

[1] *Department of Chemistry, Graduate School of Science, Osaka University, Toyonaka, Osaka 560-0043, Japan,* [2] *Department of Functional Glycomics, Life Science Research Center, Kagawa University, Kita-gun, Kagawa 761-0793, Japan*

As a first step to elucidate a role of N-glycans in development of vertebrates, we analyzed structures of the glycans expressed in early stages of zebrafish embryo. N-glycans were prepared from zebrafish embryos at several developmental stages followed by tagging with a fluorophore, 2-aminopyridine. The labeled glycans were analyzed by two modes of HPLC's. The comparison of the elution profiles of HPLC's unveil the change of the oligosaccharide structure during the development. These peaks were merely detected during 4–7 h after fertilization, however, increased from 12 h, and at 15 h a fairly amount of them was appeared. Structure analysis revealed that they were bianntenary complex-type N-glycans with or without fucose and/or bisecting *N*-acetylglucosamine residues. These results suggest that the complex-type N-glycans are concerned in some developmental event from segmentation period downward in zebrafish.
Published in 2005.

Keywords: **N-glycans, zebrafish, embryogenesis, pyridylamination**

Introduction

Glycoproteins have various kinds of glycans. N-linked glycans, one of them, were widely distributed in all eukaryote and even in some prokaryote [1,2]. The N-glycans in eukaryote are classified into several types due to their blanching structures. Complex, hybrid, and highmannose-types of N-linked glycans are commonly seen through vertebrate. Especially, complex and hybrid-types containing the *N*-acetyllactosamine structure are characteristic in vertebrate, although oligomannose-type exist in all eukaryote. Recent works clearly demonstrated that oligomannose-type glycans participated in protein folding machinery in endoplasmic reticulum (reviewed in [3]). This role of oligomannose-type glycans are corresponding to their universal distribution over eukaryote. The complex and hybrid-type glycans are not essential for viability of cultured cells [4,5]. While, they are necessary to construct of cell society in metazoa. A gene knock-out of, *N*-actylglucosaminyltransferase-I, which was a key enzyme for biosynthesis of complex and hybrid-type glycans, caused embryonic lethality in mice [6,7].

To whom correspondence should be addressed: Sumihiro Hase, Department of Chemistry, Graduate School of Science, Osaka University, 1-1 Machikaneyama, Toyonaka, Osaka 560-0043, Japan. Tel.: +81-6-6850-5380; Fax: +81-6-6850-5383; E-mail: suhase@chem.sci.osaka-u.ac.jp

Previous studies to detect stage-specific sugar chains were mainly performed using complementary probes such as antibodies and lectins. These approaches are useful to identify regional differences in expression of the glycans, however, these probes can detect only partial structures of the sugar chains. Furthermore, the probes are not comprehensively applicable to detect glycans, because most glycans are immunogenically low to prepare specific antibodies and available lectins as experimental tool are limited. On the other hand, chemical analysis of glycan structures requires a substantial amount of material, and is difficult because of their structural diversity. The other choice is a 2-dimensional sugar mapping method of pyridylamino (PA-) derivatives of glycans [8,9]. Pyridylamination of glycans has several advantages, including high sensitivity and high stability, and excellent separation by reversed-phase HPLC [9]. Moreover, a combination of the pyridylamination with a 2-dimensional sugar mapping method enables the glycan mass for analyzing comprehensively and dynamically.

During the embryogenesis, several sugar chains expressed stage-specifically on the cell surface have been reported (reviewed in 10). However, the roles of them were scarcely understood. With the aim of elucidating the role of the oligosaccharide during embryogenesis, we first identified the oligosaccharides that were expressed in a stage-specific manner. Furthermore, we analyzed the structure of these glycans using 2-dimensional sugar mapping method.

Materials and methods

Preparation of zebrafish embryo

Zebrafish were cared for and their embryos handled as described elsewhere [11]. Briefly, they were maintained in aquaria at 28.5°C, and the day-night cycle was controlled with an automatic timer (14 h light/10 h dark). Zebrafish are photoperiodic in their breeding, and produce eggs shortly after sunrise. Thus, the time when the light came on was defined as 0 h. Embryos obtained were incubated at 28.5°C in embryo medium [11]. Stages of the development of embryos were decided by morphological changes, referring to the time after fertilization.

Preparation of PA-sugar chains from embryos

Prior to the preparation of N-glycans, zebrafish embryos free of corion and yolk were lyophilized. Glycan liberation from glycoproteins and pyridylamination were performed as reported previously [12]. Briefly, lyophilized embryos were subjected to hydrazinolysis (10 h, 100°C) and N-acetylation to liberate N-glycans from glycoproteins. The glycans were tagged with a fluorophore, 2-aminopyridine by reductive-amination reaction. The excess reagents were removed by solvent extraction and ion-exchange chromatography as described before [13].

High-performance liquid chromatography

Size-fractionation HPLC was performed at 25°C on a Shodex Asahipak NH2P-50 column (4.6 × 50 mm) (Showa Denko,Tokyo) at the flow rate of 0.6 ml/min. Two eluents C and D were used as the mobile phase. Eluent C was 93% acetonitrile-3% acetic acid (v/v) titrated to pH 7.0 with aqueous ammonia, and Eluent D was 20% acetonitrile-3% acetic acid (v/v) titrated to pH 7.0 with aqueous ammonia. The column was equilibrated with Eluent C:D = 97:3 (v/v). After injecting a sample, a linear gradient elution was performed to Eluent C:D = 67:33 (v/v) in 3 min and then to 29:71 (v/v) in 32 min. PA-Glycans were detected by measuring the fluorescence (excitation wavelength, 310 nm; emission wavelength, 380 nm). The elution positions of the PA-glycans were converted into glucose unit on the basis of the elution times of PA-isomaltooligosaccharides (Takara Biomedicals, Kyoto) as described before [12].

Reversed-phase HPLC was performed using following conditions on a Cosmosil 5C18-P column (1.5 × 250 mm) (Nacalai Tesque, Kyoto) at the flow rate of 150 μl/min at 25°C. The column was equilibrated with 20 mM ammonium acetate buffer, pH 4.0, containing 0.075% 1-butanol. After injecting a sample, the concentration of 1-butanol was increased linearly to 0.4% in 90 min. Elution of PA-glycans was monitored by measuring the fluorescence (excitation wavelength, 320 nm; emission wavelength 400 nm). The elution positions of the PA-sugar chains were converted into reversed-phase scale as reported previously [14].

Two-dimensional sugar mapping

The structures of the PA-glycans were assessed by two-dimensional sugar mapping. The elution positions of more than 100 standard PA-N-linked sugar chains have already been reported, and the introduction of a reversed-phase scale made it possible to predict the elution positions even if standard PA-N-linked sugar chains were not available [14]. PA-sugar chains were separated by reversed-phase HPLC and size-fractionation HPLC, and the elution position of each sugar chain was compared with those of standard PA-sugar chains on the two-dimensional sugar map. Then each PA-sugar chain was digested with exoglycosidases, and the structures of the products were analyzed on the two-dimensional sugar map as reported previously [15].

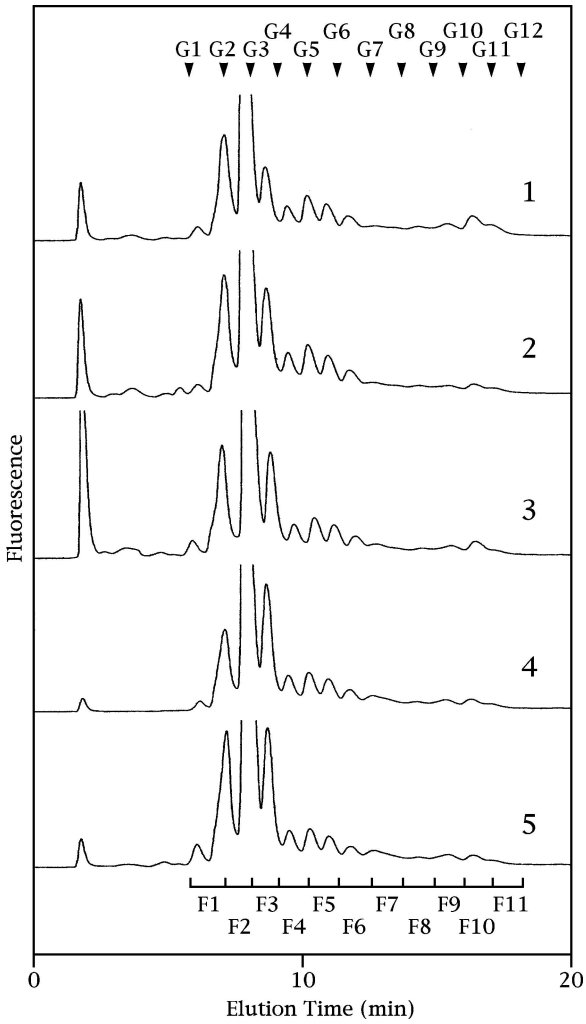

Figure 1. *Size-fractionation HPLC of PA-glycans from zebrafish embryos.* HPLC was performed on a Shodex Asahipak NH2P-50 column (4.6 × 50 mm). 1, PA-glycans obtained from 4 h embryos after fertilization; 2, 7 h; 3, 12 h; 4, 15 h; and 5, 18 h. The arrowheads G1–G12 indicate the elution positions of PA-Glucose – PA-isomaltododecasaccharides. Fractions F1–F11 were collected as indicated by the partitioned bars.

Enzymatic hydrolysis of PA-sugar chains

A PA-sugar chain was digested with 0.1 units of sialidase (*Arthrobactor ureafacience*) (Nacalai Tesque, Kyoto) in 50 μl 0.1 M ammonium acetate buffer, pH 6.0, at 37°C; with 0.5 units of jack bean β-galactosidase (Seikagaku Corp., Tokyo) in 50 μl 50 mM sodium citrate buffer, pH 3.5, at 37°C; with 0.01 units of β-N-acetylhexosaminidase (*Streptcoccus pneumoniae*) (Boehringer Mannheim, Germany) in 50 μl 50 mM ammonium acetate buffer, pH 6.0, at 37°C. The digestions were performed for 16 h and terminated by heating at 100°C for 3 min.

Results

Separation of PA-N-linked glycans from zebrafish embryos by HPLC

PA-N-linked glycans were prepared from zebrafish embryos at 4, 7, 12, 15, or 18 h after fertilization. After sialidase treatment, the PA-glycans were developed and separated into eleven fractions (F1–F11) by size-fractionation HPLC (Figure 1). Each fraction was further separated by reversed-phase HPLC. Comparison of the glycan expression patterns of the chosen developmental periods using this two-modes of HPLC approach, showed typical differences for Fractions F7 and F8. Five peaks, designated A-E, were identified whose expression changed during embryogenesis (Figures 2 and 3). Their expression was detected from 12 h after fertilization, and increased drastically in several hours. Peaks A–E were isolated to analyze their structures. Both the Peaks A and B were eluted at 54.9 reversed-phase scale and 8.0 glucose units on size-fractionation HPLC. These values were corresponding to those of Sugar chain 6 (Tables 1 and 2), which is bianntenary PA-N-glycan. Their position shifted to 49.5 reversed-phase scale and 6.4 glucose units by β-galactosidase digestion. On subsequent digestion with *N*-acetyl-β-hexosaminidase a peak at 42.6 reversed-phase scale and 4.5 glucose units was observed. These values coincided with PA-glycan 3 and 1. From these results

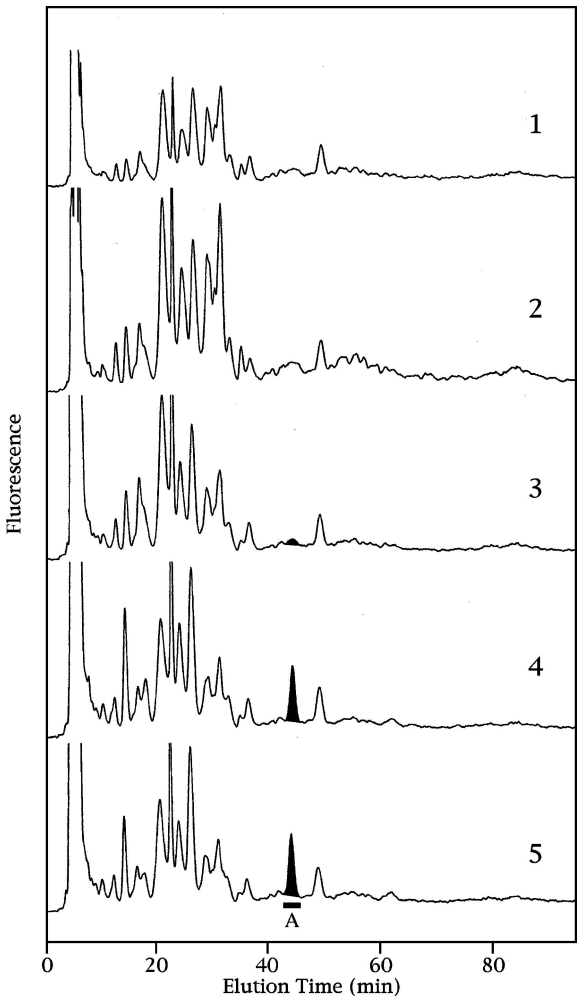

Figure 2. *Reversed-phase HPLC of Fraction F7.* HPLC was performed on a Cosmosil 5C18P column (1.5 × 250 mm). For numerals, see the legend to Figure 1. Fraction A was pooled as indicated by the thickbar.

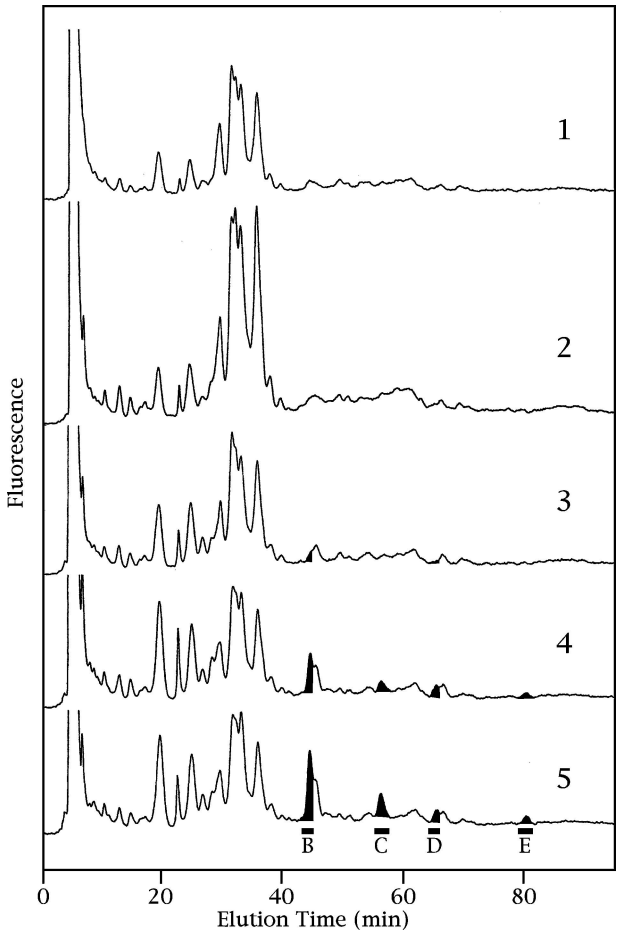

Figure 3. *Reversed-phase HPLC of Fraction F8.* HPLC was performed on a Cosmosil 5C18P column (1.5 × 250 mm). For numerals, see the legend to Figure 1. Fractions B–E were pooled as indicated by the thick bars.

Table 1. Structure, designations and elution positions of the standard PA-glycans.

Structure	*Sugar chain*	HPLC	
		Reversed phase[a]	*Size-fractionation*[b]
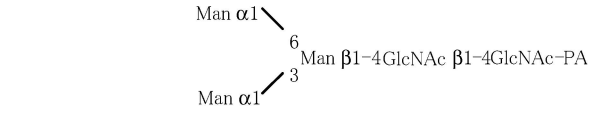	1	43.0	4.5
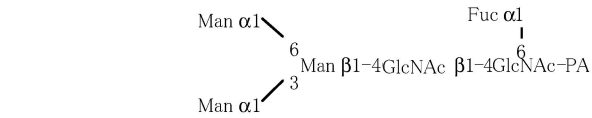	2	52.5	4.9
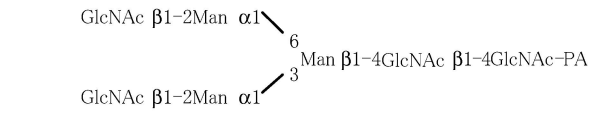	3	49.4	6.3
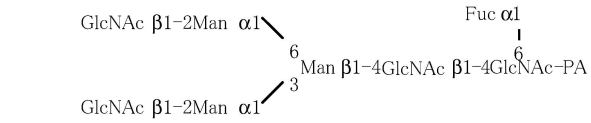	4	59.2	6.6
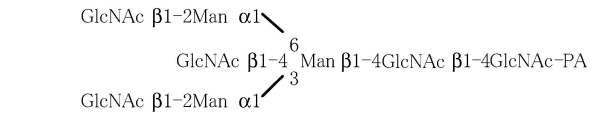	5	65.4	6.7
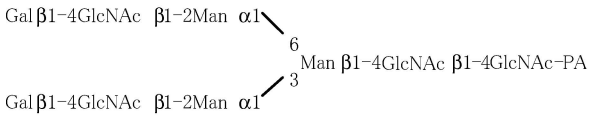	6	54.5	7.8
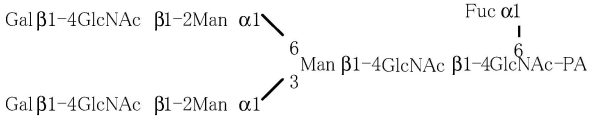	7	63.6	8.1
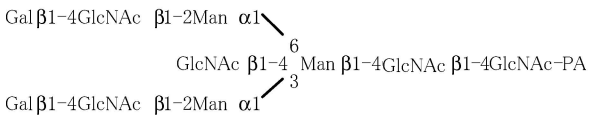	8	70.5	8.2
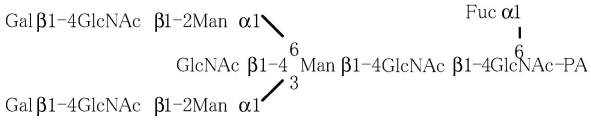	9	80.0	8.5

[a]The reversed phase scale data are from reference 11.
[b]Glucose unit.

on the 2-dimensional HPLC map, the structure of Peak A and B was estimated as Galβ1-4GlcNAcβ1-2Manα1-6(Galβ1-4GlcNAcβ1-2Manα1-3)Manβ1-4GlcNAcβ1-4GlcNAc-PA. The Peak C was eluted at 63.8 reversed-phase scale and 8.3 glucose units on size-fractionation HPLC. These values were corresponding to those of Sugar chain 7, fucosylbianntenary PA-N-glycan. Its elution position shifted to 59.2 reversed-phase scale and 6.7 glucose units by β-galactosidase digestion. Subsequent digestion with N-acetyl-β-hexosaminidase a peak at 52.1 reversed-phase scale and 4.9 glucose units was appeared. These values coincided with Sugar chain 4 and 2. Based on these results, the structure of Peak C was estimated as Galβ1-4GlcNAcβ1-2Manα1-6(Galβ1-4GlcNAcβ1-2Manα1-3)Manβ1-4GlcNAcβ1-4(Fucα1-6)GlcNAc-PA. The Peak D was eluted at 70.6 reversed-phase scale and 8.1 glucose units on size-fractionation HPLC. These values were corresponding to those of Sugar chain 8. The elution position shifted to 64.7 reversed-phase scale and 6.6 glucose units by β-galactosidase

Table 2. Two dimensional HPLC analysis combined with sequential glycosidase digestion of Peak A–E

		HPLC		
Peak	*Successive glycosidase digestion*	*Reversed-phase*[a]	*Size-fractionation*[b]	*Estimated sugar chain*[c]
A	No treatment	54.9	8.0	6
	β-Galactosidase	49.5	6.4	3
	β-*N*-Acetylhexosaminidase	42.6	4.5	1
B	No treatment	54.5	8.0	6
	β-Galactosidase	49.5	6.4	3
	β-*N*-Acetylhexosaminidase	42.6	4.5	1
C	No treatment	63.8	8.3	7
	β-Galactosidase	59.2	6.7	4
	β-*N*-Acetylhexosaminidase	52.1	4.9	2
D	No treatment	70.6	8.1	8
	β-Galactos idase	64.7	6.6	5
E	No treatment	80.0	8.3	9

[a]The reversed-phase scale are calculated as described previously (11).
[b]Glucose unit.
[c]Corresponding structures are listed in Table 1.

Table 3. Proposed structures for PA-N-linked glycans appeared at segmentation period of zebrafish embryo

Fraction	*Proposed structure*	*Relative amount*
A and B	Galβ1-4GlcNAcβ1-2Manα1↖ 6 3 Manβ1-4GlcNAcβ1-4GlcNAc-PA; Galβ1-4GlcNAcβ1-2Manα1↗	1
C	Galβ1-4GlcNAcβ1-2Manα1↖ Fucα1 6 6 Manβ1-4GlcNAcβ1-4GlcNAc-PA; Galβ1-4GlcNAcβ1-2Manα1↗ 3	0.2
D	Galβ1-4GlcNAcβ1-2Manα1↖ GlcNAcβ1-4 6 Manβ1-4GlcNAcβ1-4GlcNAc-PA; Galβ1-4GlcNAcβ1-2Manα1↗ 3	0.1
E	Galβ1-4GlcNAcβ1-2Manα1↖ Fucα1 GlcNAcβ1-4 6 6 Manβ1-4GlcNAcβ1-4GlcNAc-PA; Galβ1-4GlcNAcβ1-2Manα1↗ 3	0.06

digestion. These values coincided with Sugar chain 5. The β-galactosidase digest of Peak D was too small to be analyzed further. The Peak E was eluted at 80.0 reversed-phase scale and 8.3 glucose units on size-fractionation HPLC. These values were corresponding to those of Sugar chain 9. This peak was too small to be analyzed further by exoglycosidase digestion. From these results, structures of Peaks D and E were estimated as Galβ1-4GlcNAcβ1-2Manα1-6(Galβ1-4GlcNAcβ1-2Manα1-3)(GlcNAcβ1-4)Manβ1-4GlcNAcβ1-4GlcNAc-PA and Galβ1-4GlcNAcβ1-2Manα1-6(Galβ1-4GlcNAcβ1-2Manα1-3)(GlcNAcβ1-4)Manβ1-4GlcNAcβ1-4(Fucα1-6)GlcNAc-PA, respectively. Differences of the values between samples and standard sugar chains were less than 0.9% in reversed-phase scale and 2.5% in glucose units of size-fractionation HPLC. These small differences were within experimental error. The proposed structures are summarized in Table 3. On the other hand, oligomannose-type N-glycans were detected in fairly amount through developmental periods we tested. Especially, Manα1-6(Manα1-3)Manα1-6(Manα1-3)Manβ1-4GlcNAcβ1-4GlcNAc-PA and Manα1-2Manα1-6(Manα1-2Manα1-3)Manα1-6(Manα1-2Manα1-2Manα1-3)Manβ1-4GlcNAcβ1-4GlcNAc-PA were dominant structures throughout the stages. The oligomannose-type glycans containing 6-8 mannnose residues were also detected. Their major structure were Manα1-2Manα1-6(Manα1-3)Manα1-6(Manα1-2Manα1-2Manα1-3)Manβ1-4GlcNAcβ1-4GlcNAc-PA, Manα1-2Manα1-6(Manα1-3)Manα1-6(Manα1-2Manα1-3)Manβ1-4GlcNAcβ1-4GlcNAc-PA and Manα1-6(Manα1-3)Manα1-6(Manα1-2Manα1-3)Manβ1-4GlcNAcβ1-4GlcNAc-PA. These and its isomeric

structures of them were not significantly altered in any period.

Discussion

In this study, N-glycans expressed in several developmental stages were compared with each other. Whereas amounts of most major N-linked glycans were not significantly altered in the embryonic period we tested, the expression of several glycans was drastically changed during segmentation period. The peaks of these glycans were scarcely detected until 7 h after fertilization, and then greatly increased by 15 h. The analysis using a two-dimensional sugar mapping and glycosidase digestion made clear that they were a diantennary structure and its derivatives with α1-6 linked fucose and/or bisecting GlcNAc. They are common structures of complex-type glycans in vertebrates.

N-Acetylglucosaminyltransferase I (GnTI) catalyzes the key reaction in the formation of complex type and hybrid type N-linked glycans. Mice lacking the GnTI gene die between embryonic days 9.5 and 10.5 [6,7]. Therefore, the glycans biosynthetically regulated by GnTI in this period may critically involve in embryogenesis. This stage of mouse embryo is roughly corresponded to that of 12–15 h after fertilization in the case of zebrafish. Thus the complex-type glycans we observed in this study might participate in some developmental event, although a physiological role of GnTI in zebrafish is unknown. As a next step, identification of the glycoprotein(s) bearing the complex-type glycans are necessary for further elucidation of biological function of the glycans in embryo.

A sialidase digestion was carried out prior to HPLC analysis in this study, it is unknown whether the diantennary glycans observed were originally sialylated or not. It is known that complex-type sugar chains with negative charges were important in neural development ([16], reviewed in [17]). Further study is needed to determine whether these glycans serve as the carrier of negative charge.

Acknowledgment

This study was supported in part by the Research for the Future Program of the Japan Society for the Promotion of Science, and by a grant for Research on Health Sciences Focusing on Drug Innovation.

References

1 Wacker M, Linton D, Hitchen PG, Nita-Lazar M, Haslam SM, North SJ, Panico M, Morris HR, Dell A, Wren BW, Aebi M, N-linked glycosylation in *Campylobacter jejuni* and its functional transfer into *E. coli, Science* **298**, 1790–3 (2002).

2 Young NM, Brisson JR, Kelly J, Watson DC, Tessier L, Lanthier PH, Jarrell HC, Cadotte N, St Michael F, Aberg E, Szymanski CM, Structure of the N-linked glycan present on multiple glycoproteins in the Gram-negative bacterium, *Campylobacter jejuni*, *J Biol Chem* **277**, 42530–9 (2002).

3 Helenius A, Aebi M, Intracellular functions of N-linked glycans, *Science* **291**, 2364–9 (2001).

4 Gottlieb C, Baenziger J, Kornfeld S, Deficient uridine diphosphate-N-acetylglucosamine:glycoprotein N-acetylglucosaminyltransferase activity in a clone of Chinese hamster ovary cells with altered surface glycoproteins, *J Biol Chem*, **250**, 3303–9 (1975).

5 Stanley P, Narasimhan S, Siminovitch L, Schachter H, Chinese hamster ovary cells selected for resistance to the cytotoxicity of phytohemagglutinin are deficient in a UDP-N-acetylglucosamine-glycoprotein *N*-acetylglucosaminyltransferase activity, *Proc Natl Acad Sci USA* **72**, 3323–7 (1975).

6 Metzler M, Gertz A, Sarkar M, Schachter JW, Marth JD. (1994) Complex asparagine-linked oligosaccharides are required for morphogenic events during post-implantation development, *EMBO J* **13**, 2056–65.

7 Ioffe E, Stanley P. Mice lacking N-acetylglucosaminyltransferase I activity die at mid-gestation, revealing an essential role for complex or hybrid N-linked carbohydrates. *Proc Natl Acad Sci USA* **91**, 728–32 (1994).

8 Hase S, Ikenaka T, Matsushima Y, Structural analysis of oligosaccharides by tagging of the reducing end sugars with a fluorescent compound, *Biochem Biophys Res Commun* **85**, 257–63 (1978).

9 Hase S, Ikenaka T, Matsushima Y. A highly sensitive method for analyses of oligosaccharides by tagging of the reducing end sugars with a fluorescent compound, *J Biochem* **9**, 407–14 (1981).

10 Muramatsu T. Developmentally regulated expression of cell surface carbohydrates during mouse embryogenesis, *J Cell Biochem* **36**, 1–14 (1988).

11 Streisinger G, *The Zebrafish Book*, edited by Westerfield M (University of Oregon Press, Eugene, OR, 1995).

12 Natsuka S, Hase S, Analysis of N- and O-glycans by pyridylamination, *Methods Mol Biol* **76**, 101–13 (1998).

13 Yanagida K, Natsuka S, Hase S, A pyridylamination method aimed at automatic oligosaccharide Analysis of N-linked Sugar Chains, *Anal Biochem* **274**, 229–34 (1999).

14 Yanagida K, Ogawa H, Omichi K, Hase S, Introduction of a new scale into reversed-phase high performance liquid chromatography of pyridylamino sugar chains for structural assignment, *J Chromatogr A* **800**, 187–98 (1998).

15 Makino Y, Omichi K, Hase S, Analysis of sugar chain structures from the reducing end terminal by combining partial acid hydrolysis and a two-dimensional sugar map, *Anal Biochem* **263**, 172–179, (1998).

16 Finne J, Finne U, Deagostini-Bazin H, Goridis C, Occurrence of α2-8 linked polysialosyl units in a neural cell adhesion molecule, *Biochem Biophys Res Commun*, **112**, 482–7 (1983).

17 Schachner M, Martini R, Glycans and the modulation of neural-recognition molecule function, *Trends Neurosci*, **18**, 183–91 (1995).

Received 22 June 2004; revised 17 Sept. 2004; accepted 20 Sept. 2004